Mol. Cryst. Liq. Cryst., Vol. 410, pp. 83/[611]–93/[621], 2004

ISSN: 1542-1406 print/1563-5287 online
DOI: 10.1080/15421400490436124

Taylor & Francis
Taylor & Francis Group

MECHANISM OF FORMATION OF THREE DIMENSIONAL STRUCTURES OF PARTICLES IN A LIQUID CRYSTAL

John L. West, Ke Zhang, Guangxun Liao, and Anatoliy V. Glushchenko*
Liquid Crystal Institute, Kent State University, Kent, Ohio 44242, USA

Yuri Reznikov
Institute of Physics, Prosect Nauky 46, Kyiv 03039, Ukraine

Denis Andrienko
Max-Plank Institute, Ackermannweg, 10, Mainz 55128, Germany

Michael P. Allen
Department of Physics and Center for Scientific Computing, University of Warwick, CV4 7AL, United Kingdom

In this work we report methods of formation of three-dimensional structures of particles in a liquid crystal host. We found that, under the appropriate conditions, the particles are captured and dragged by the moving isotropic/nematic front during the phase transition process. This movement of the particles can be enhanced significantly or suppressed drastically with the influence of an electric field and/or with changing the conditions of the phase transition, such as the rate of cooling. As a result, a wide variety of particle structure can be obtained ranging from a fine-grained cellular structure to stripes of varying periods to a course-grained "root" structure. Changing the properties of the materials, such as the size and density of the particles and the surface anchoring of the liquid crystal at the particle surface, can also be used to control the morphology of the three-dimensional particle network and adjust the physical properties of the resulting dispersions. These particle structures may be used to affect the performance of LCD's much as polymers have been used in the past.

Keywords: drag of particles; liquid crystal; nematic-isotropic interface

This work was supported through ALCOM grant DMR 89–20147.

*Corresponding author. Tel.: +1-330-672-2581, Fax.: +1-330-672-2796, E-mail: johnwest@lci.kent.edu

1. INTRODUCTION

Colloidal dispersions of small particles in nematic liquid crystals are a novel, interesting type of soft matter. The difference from ordinary colloids arises from the orientational ordering of the liquid crystal molecules and the resulting structure in the colloid. Topological defects [1,2] and additional long-range forces between the colloidal particles [3] are immediate consequences of this ordering. The nematic-induced interparticle interaction brings a new range of effects to the system: supermolecular structures [4,6], cellular structures [7,8], and even a soft solid [9] can be observed. Colloidal dispersions in liquid crystals also have a wide variety of potential applications [10].

A range of problems also arises in nematic colloidal dispersions. The nematic ordering makes it difficult to suspend small particles in a liquid crystal host [11]. Particles often segregate into agglomerates distributed non-uniformly in the cell. The resulting spatial distribution of the particles is difficult to control. Our research therefore explores the factors that affect the spatial distribution of these particles.

In our previous work we reported the first demonstration of drag on colloidal particles by a moving nematic-isotropic (NI) interface [12]. We calculated a critical radius above which the particles cannot be captured by the moving interface. We showed that this critical radius is sensitive to the viscous properties of the host liquid crystal, the value of the anchoring coefficient of the liquid crystal on the particle surface, and the velocity of the moving interface.

In the experimental work reported here we demonstrate the methods used to control the spatial distribution of particles of different sizes in a liquid crystal cell. We show that an electric field and/or changing the conditions of the nematic-isotropic phase transition, such as the rate of cooling, can be used to control the morphology of the three-dimensional particle network and adjust the physical properties of the resulting dispersions and displays.

2. EXPERIMENTS

In order to understand how the particles are moved by the nematic-isotropic transition front we used particles of different size as well as particles made of different materials. First we used nearly monodisperse spheres of silica ($R = 0.005\,\mu m$). To directly observe the movement of particles and to demonstrate how we control the spatial distribution of particles in an anisotropic colloidal suspension, we used large polymer particles, $R = 8\,\mu m$. These particles are used as spacers in the LCD

industry (Micropearl SP, made of cross-linked copolymer with divinylbenzene as a major component, $\rho = 1.05$–$1.15\,\mathrm{g{\cdot}cm^{-3}}$). In all cases, particles were dispersed at concentrations of $\varphi = 1$–$5\,\mathrm{wt\%}$, in the liquid crystal 5CB at room temperature. The sample was subjected to ultrasound in order to uniformly disperse the particles in 5CB.

The homogeneous mixture of the liquid crystal and particles was deposited between two polyimide-covered ITO-glass substrates. The polyimides were selected to provide either planar or homeotropic orientation of the 5CB liquid crystal. The cell thickness was large enough (20–50 μm) to assure the unimpeded passage for the particles.

One of the edges of the cell was placed onto a temperature controlled hot-stage, as shown in Figure 1. Such a configuration provided a gradient of the temperature through the entire area of the cell. The distribution of the temperature gradient depended on the balance between the temperature of the hot-stage and room temperature. This produced a nematic-isotropic transition interface parallel to the heated edge of the cell. Any changes of the hot-stage temperature led to a change in the position of the interface in the cell. The speed of the temperature change, that could be controlled with high precision (0.01 deg/min), determined the speed of the interface. An optical microscope provided with a CCD camera and video recorder was used to observe the cell.

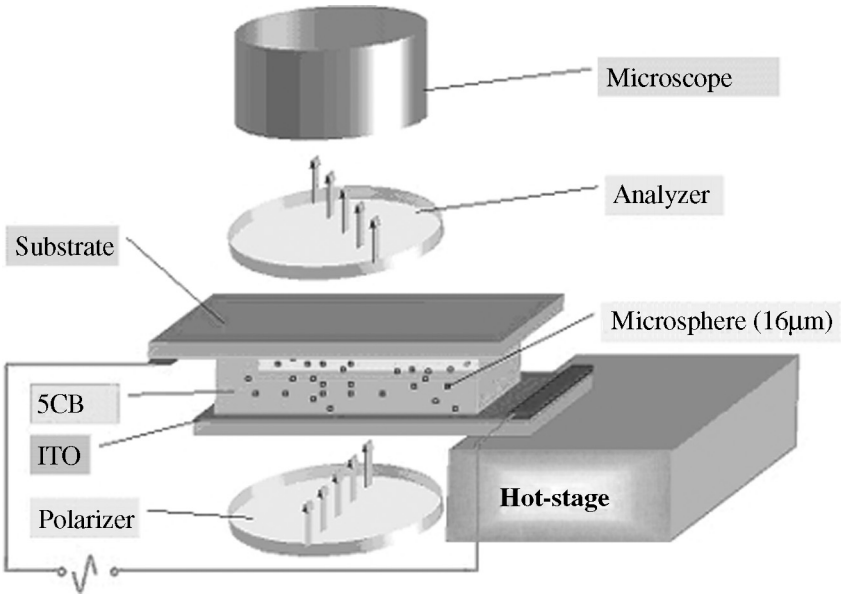

FIGURE 1 Experimental set-up.

3. RESULTS AND DISCUSSION

First, the homogeneous suspension was heated into the isotropic state (Fig. 2a) and then was cooled to a temperature below $T_{N\text{-}I}$. Depending on the rate of cooling, we observed different structures. Fast quenching to room temperature (cooling rate $10^{\circ}\text{C}\cdot\text{min}^{-1}$) resulted in phase transition and formation of a cellular structure, with particle-free nematic domains separated by particle-rich regions, (Fig. 2b). The properties of these structures have been reported previously [7–9]. Decreasing the cooling rate, we observed formation of a striped structure (Fig. 2c). The particle-rich regions no longer formed a cellular structure but were arranged in a set of stripes, separated by particle-free regions. Using optical microscope images we postulate that we have large nematic and isotropic domains separated by a moving interface. The direction of the stripes is parallel

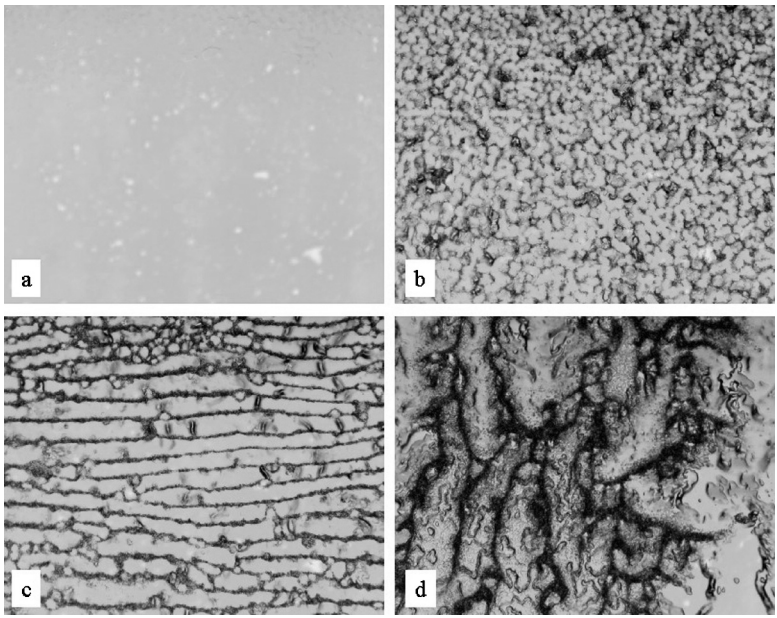

FIGURE 2 Polarized microscopy images of different structures, depending on the cooling rate: (a) colloidal particles are dispersed homogeneously in the isotropic phase; (b) *cellular* structure: cooling rate $= 10^{\circ}\text{C}\cdot\text{min}^{-1}$; (c) *stripes*: cooling rate $= 0.1^{\circ}\text{C}\cdot\text{min}^{-1}$, velocity of the interface $v \approx 3\,\mu\text{m}\cdot\text{sec}^{-1}$; (d) *root* structure: cooling rate $= 0.01^{\circ}\text{C}\cdot\text{min}^{-1}$, $v \approx 0.5\,\mu\text{m}\cdot\text{sec}^{-1}$. Silica particles, $R = 0.005\,\mu\text{m}$, concentration $\varphi = 1\,\text{wt}\%$. The N-I interface is moving from the top of the pictures downwards. The long side of the images is 1 mm.

to the moving interface (the interface was moving downward in the picture in the geometry depicted in Figure 2). The spatial period of the striped structure depended on the cooling rate, as well as on the particle size. Increasing the particle size, as well as decreasing the cooling rate, resulted in an increase of the spatial period. Interestingly the stripes do not appear using considerably larger silica particles, $R > 0.5\,\mu m$. Also, decreasing the cooling rate resulted in a chaotic merging of stripes and formation of a "root"-like pattern, (Fig. 2d). These results indicate that the particles are pushed by the moving nematic-isotropic phase transition front.

Using optical microscopy we were able to directly observe the movement of larger ($R = 8\,\mu m$) but less dense polymer spheres [13]. We could see these particles being moved by an advancing nematic to isotropic phase boundary. Figure 3 shows pictures of this moving front taken at different times. Clearly the particles are pushed by this advancing front, remaining in the isotropic phase. In Figure 4 we demonstrated the ability to control the spatial distribution of the particles by changing the cooling rate. An advancing line of particles, pushed by the $T_{N\text{-}I}$ boundary could be dropped by increasing the cooling rate and thus the velocity of the moving boundary (Fig. 4c). This results in formation of a stripe. Subsequent slowing of the cooling resumes collection of particles at the interface (Fig. 4d).

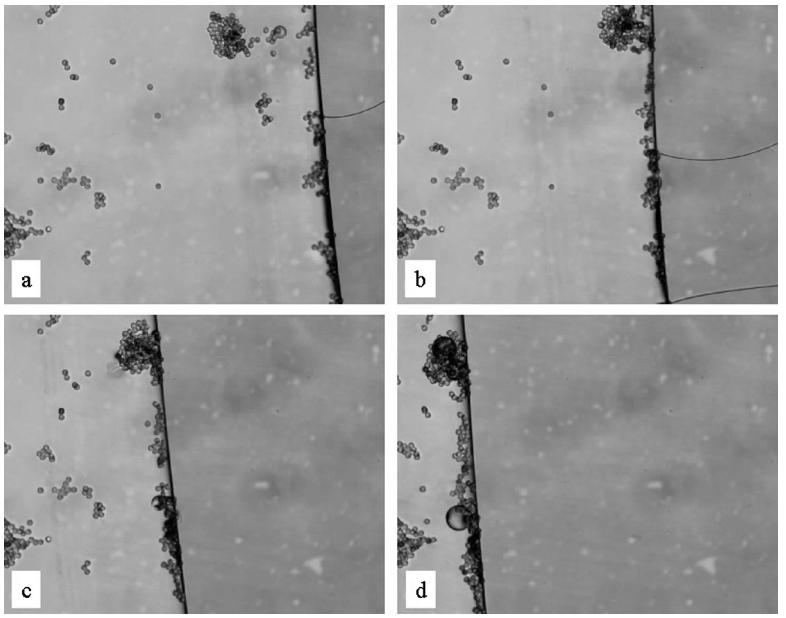

FIGURE 3 Snapshots of the moving nematic-isotropic interface made between parallel polarizers taken with the time interval $\Delta t = 6\,min$.

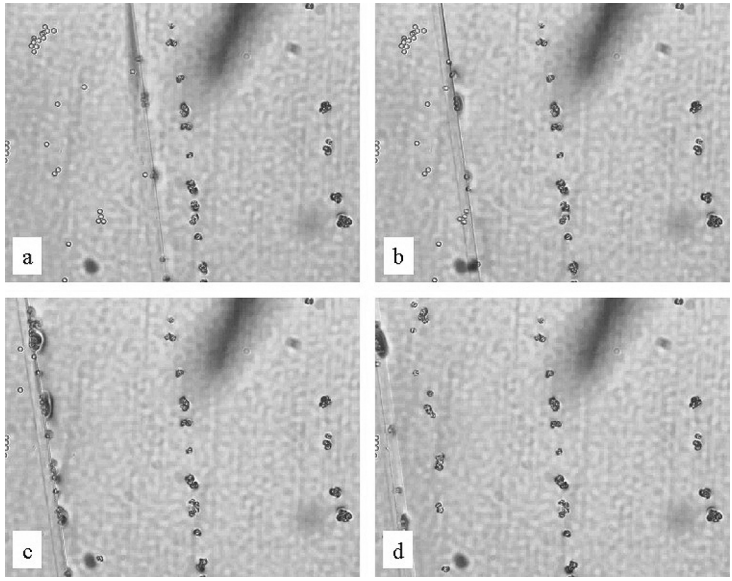

FIGURE 4 Formation of stripes of particles by moving the nematic-isotropic interface.

We have found that the nematic-isotropic interface can also drag the particles in the opposite direction, i.e. upon heating the cell. But in this case the movement of the interface must be much slower to move the particles. Figure 5 demonstrates merging two stripes into one using this inverse movement.

An electric field can be used to precisely form particle structures. We demonstrated that with an electric field applied high enough to align the nematic, the particles can be dragged by a higher velocity interface. This change in the maximum velocity provides another means to precisely drop particles. For example, we prepared a cell with homeotropic boundary conditions and applied a normally aligned electric field to the entire area of the cell (Fig. 6). The cell was cooled at a rate of 10 deg/min. With a field of 1 V/μ applied all the particles were pushed by the interface. We formed stripes by switching off the electric field for a short time. This reduced the effective elasticity of the liquid crystal (Fig. 6a). As a result, the particles and their aggregates were dropped (Fig. 6b). Successive application of the electric field allows us to form designed particles structure.

A simple analysis accounts for these experimental observations. We considered several mechanisms which contribute to the total drag force acting on a particle at a N-I interface. First, the surface tension coefficient might differ at the particle-nematic or particle-isotropic part of the

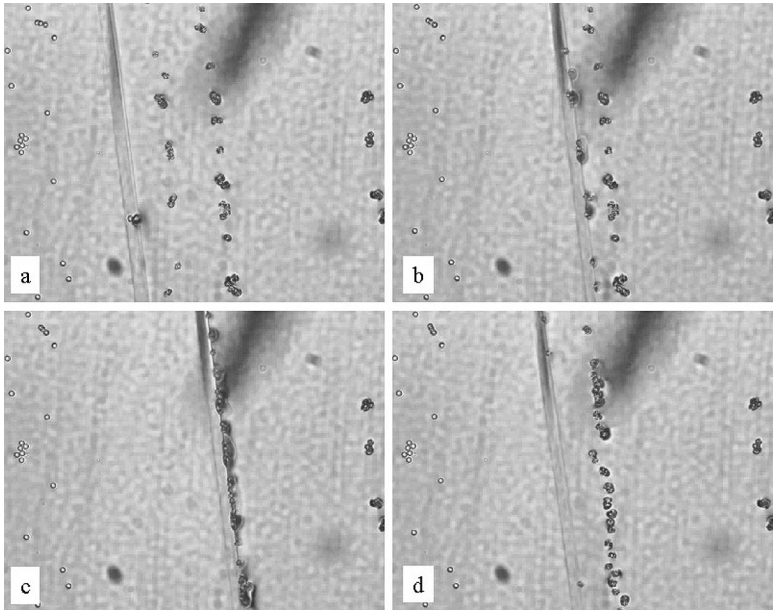

FIGURE 5 The merging process of two stripes into one.

interface. An additional pressure caused by the curvature can be given by $P = 2\sigma/R$, where R is the radius of the curvature (in our case it is the radius of the particle) and σ is the surface tension coefficient. This pressure contributes to the total drag force as $F_\sigma = 2\pi(\sigma_N - \sigma_I) \cdot R \cdot [1 - (d/R)^2]$, with the amplitude growing linearly with the droplet radius. Here d is the distance from the particle center to the interface.

Second, the particle creates long-range distortions of the director in a nematic phase. To minimize the elastic distortion energy, the nematic expels particles into the isotropic phase. The elastic forces have two origins: due to the director deformations in the bulk nematic and due to the anchoring of the director at the particle surface. An estimation of these contributions can be done by dimensional analysis. For the surface contribution, the only combination which has dimension of force is WR, where W is the anchoring coefficient. Therefore, the surface contribution to the drag force is proportional to WR, $F_s = WRg_s(d/R)$, where $g_s(x)$ is a dimensionless function of the penetration depth, d/R. One can have two different situations for the bulk contribution. For *weak* anchoring, $WR/K << 1$, the bulk contribution is proportional to the squared distortion of the director, $\beta_0 \sim WR/K$ [14]. Now W^2R^2/K has the dimension of force, yielding $F_b = W^2R^2/Kg_b(d/R)$ In contrast, in the case of strong anchoring,

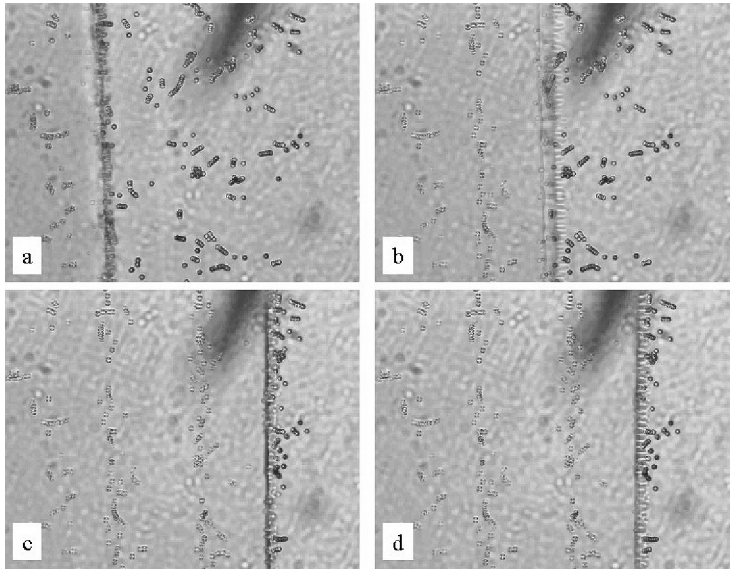

FIGURE 6 Formation of the stripes of particles by the movement of the nematic-isotropic interface and periodic action of an electric field. The nematic phase is on the left size of the pictures.

$WR/K >> 1$, the anchoring does not enter the elastic contribution, and $F_b = Kg_b(d/R)$. For 5CB, and typical values of the anchoring energy, $W \sim 10^{-3} - 10^{-4}$ dyn cm^{-1}, $WR/K << 1$ for silica particles and $WR/K \sim 1$ for polymer particles. Therefore, for silica particles, we have the weak anchoring regime. In contrast, polymer particles provide strong anchoring of the director. We also note that, when particles agglomerate, the effective radius increases and we have a strong anchoring regime even for small particles.

Finally, we have a frictional drag contribution, which, in the first approximation, is given by the Stokes formula, $F_\eta = -6/\pi R\eta v$ [15]. The total drag on the particle is the sum of the following contributions: $F_{drag} = F_\sigma + F_b + F_s + F_\eta$.

Solution of Newton's equations of motion with F_{drag} as a force completes the description of the particle dynamics. The maximal radius can be estimated from the conservation of linear momentum. To capture a particle of mass m, the interface has to transfer to it a linear momentum mv. If we assume that the particle does not move (or it moves much slower than the interface, which is valid for massive particles) then the total linear momentum transferred to the particle reads

$$mv = \int_{t_1}^{t_2} F_{drag}\, dt = \frac{1}{v}\int_{-R}^{R} F_{drag}(x)\, dx \tag{1}$$

Here we assumed that the interface touches the particle at time t_1 and leaves it at time t_2, $x = vt$. Substituting F_{drag} we obtain

$$R_{\max} = \frac{\frac{8}{3}\pi\Delta\sigma + \delta_s W - 6\pi\eta\Delta r}{\frac{4}{3}\pi\rho v^2 - \delta_b W^2/K} \tag{2}$$

where δ_i are geometrical constants, ρ is the density of the particle, Δr is the final displacement of the particle due to the drag force.

Several important conclusions can be drawn. First, if the particle is too big, the moving interface is not able to transfer sufficient linear momentum to it. Only particles with $R < R_{max}(v, W, \sigma)$ will be captured by the interface. From Eq. (2) one can see that $R_{max} \sim v^{-2}$, i.e. only a slowly moving interface is able of capturing the particles. The estimate of this velocity gives $v \sim W/(K\rho)^{-1/2} \sim 1\,\mathrm{mm\ sec}^{-1}$. This is of the order of the limiting velocity for the cellular structure we observed in our experiments: if the interface moves more slowly, then stripes appear, otherwise the cellular structure forms (see Fig. 2).

The main conclusion is that R_{max} is a function of the material parameters, i.e. can be effectively controlled, for example, by changing the surface treatment of the particles (anchoring energy W). Increase in the anchoring energy leads to an increase of R_{max}. Moreover, strong enough anchoring favors formation of a defect near the particle [2,4], contributing to an even higher energetic barrier created by elastic forces.

On the other hand, if the particle is captured by the interface, the elastic force scales as R^2, and the opposing viscous drag scales as R. Therefore, there is a minimal radius, R_{min}, starting from which particles will be dragged by the interface. If the particle is dragged by the interface at a constant speed, then $F_{drag} = 0$, yielding

$$R_{\min} = \frac{6\pi\eta v - 2\pi\Delta\delta - \gamma_s W}{\gamma_b W^2/K} \tag{3}$$

where $\gamma_1 = g_i(0)$ are constants. Equation (3) implies that, in order to be moved by the interface, the particles have to be big enough. Only in this case can elastic forces overcome viscous drag. Substituting values typical for 5CB and using the slowest cooling rate, we obtain $R_{min} \sim 0.01\,\mu\mathrm{m}$ which qualitatively agrees with the minimum size of silica particles we were able to move.

To explain formation of the striped structure, we observe that aggregates grow while they are dragged by the interface, capturing more

and more particles. Eventually they merge and form a stripe. Attractive interactions between the aggregates (such as depletion-like or due to the presence of defects between them) help them to merge into a continuous stripe at the interface. At this point the interface must push a continuous wall of particles through the stationary liquid. We postulate that the large force required results in the interface dropping the stripe and beginning to form a new stripe.

In a more quantitative model we consider a single spherical aggregate. When such an aggregate moves, it captures more and more particles, growing in size. The anchoring parameter WR/K also increases and we switch from the weak anchoring to the strong anchoring regime. The bulk elastic contribution is then proportional to the elastic constant K and the elastic force is no longer growing as R^2. Therefore, at some R_c, the friction drag overcomes the elastic contribution and the aggregate breaks through the interface. The aggregate is dropped and the particles start to accumulate again. The condition $F_{drag} = 0$ gives the critical size of the aggregate

$$R_c = \frac{\gamma_b K}{6\pi\eta v - 2\pi\Delta\sigma} \tag{4}$$

which is about 1 μm for typical experimental values.

From conservation of mass one can show that the radius of the aggregate increases linearly with time until it reaches R_c,

$$R = R_0 + \frac{1}{4}\varphi\frac{\rho_{LC}}{\rho_a}vt \tag{5}$$

Here R_0 is the initial radius of the aggregate, ρ_a is the density of the aggregate. Therefore, the distance between aggregates is given by

$$\lambda \approx 4\varphi^{-1}\frac{\rho_a}{\rho_{LC}}R_c \tag{6}$$

and is of the order of 0.1 mm. As expected, this is in a quantitative agreement with the observed distance between stripes area in Figure 2. To derive a more precise theory for the formation of stripes, we need to take into account the interaction of aggregates, presence of defects, etc. The complexity of this problem increases significantly, and is beyond the scope of this paper.

4. CONCLUSIONS

In this work we report methods of formation of three-dimensional structures of particles in a liquid crystal host. We found that, under the

appropriate conditions, the particles are captured and dragged by the moving isotropic/nematic front during the phase transition process. This movement of the particles can be enhanced significantly or suppressed drastically with the influence of an electric field and/or with changing the conditions of the phase transition, such as the rate of cooling. As a result, a different variety of particle formations can be obtained: from a fine-grained cellular structure to stripes of varying periods to a course-grained "root" structure. Changing the properties of the materials, such as the size and density of the particles and the surface anchoring of the liquid crystal at the particle surface, can also be used to control the morphology of the three-dimensional particle network and adjust the physical and related electro-optical properties of the resulting dispersions.

REFERENCES

[1] Stark, H. (1999). Director field configurations around a spherical particle in a nematic liquid crystal. *Euro. Phys. J B.*, *10*, 311–321.
[2] Lubensky, T. C., Pettey, D., Currier, N., & Stark, H. (1998). Topological defects and interactions in nematic emulsions. *Phys. Rev. E.*, *57*, 610–625.
[3] Lev, B. I. & Tomchuk, P. M. (1999). Interaction of foreign microdroplets in a nematic liquid crystal and induced supermolecular structures. *Phys. Rev. E.*, *59*, 591–602.
[4] Poulin, P., Stark, H., Lubensky, T. C., & Weitz, D. A. (1997). Novel colloidal interactions in anisotropic fluids. *Science.*, *275*, 1770–1773.
[5] Poulin, P. & Weitz, D. A. (1998). Inverted and multiple nematic emulsions. *Phys. Rev. E.*, *57*, 626–637.
[6] Loudet, J., Barois, P., & Poulin, P. (2000). Colloidal ordering from phase separation in a liquid- crystalline continuous phase. *Nature*, *407*, 611–613.
[7] Anderson, V. J., Terentjev, E. M., Meeker, S. P., Crain, J., & Poon, W.C. K. (2001). Cellular solid behavior of liquid crystal colloids. 1. Phase separation and morphology. *Euro. Phys. J. E.*, *4*, 11–20.
[8] Anderson, V. J. & Terentjev, E. M. (2001). Cellular solid behavior of liquid crystal colloids. 2. Mechanical properties. *Euro. Phys. J. E.*, *4*, 21–28.
[9] Meeker, S. P., Poon, W. C. K., Crain, J., & Terentjev, E. M. (2000). Colloid—liquid-crystal composites: An unusual soft solid. *Phys. Rev. E.*, *61*, R6083–R6086.
[10] Russel, W., Saville, D., & Schowalter, W. (1989). Colloidal Dispersions. Cambridge University Press.
[11] Poulin, P., Raghunathan, V. A., Richetti, P., & Roux, D. (1994). On the dispersion of latex particles in a nematic solution. *J. Phys. II.*, *4*, 1557–1569.
[12] West, J. L., Glushchenko, A., Liao, G., Reznikov, Yu., Andrienko, D., & Allen, M. (2002). Drag on particles in a nematic suspension by a moving nematic-isotropic interface. *Phys. Rev. E.*, *66*, 0127021–0127024.
[13] The real time movie can be downloaded from: http://orbis.kent.edu:8080/ramgen/LCI/film5.rm.
[14] Kuksenok, O. V., Ruhwandl, R. W., Shiyanovskii, S. V., & Terentjev, E. M. (1996). Director structure around a colloid particle suspended in a nematic liquid crystal. *Phys. Rev. E.*, *54*, 5198–5203.
[15] Billeter, J. L. & Pelcovits, R. A. (2000). Defect configurations and dynamical behavior in a Gay-Berne nematic emulsion. *Phys. Rev. E.*, *62*, 711–717.